

Robust Time Reversal-based Transmit Optimization for Green Heterogeneous Networks

Ha-Vu Tran¹, Dac-Binh Ha², Hieu Nguyen³, Een-Kee Hong¹

¹*School of Electronic and Information, Kyung Hee University,
South Korea*

²*Faculty of Electrical and Electronics Engineering, Duy Tan University,
Vietnam*

³*School of Electrical and Electronic Engineering, Nanyang Technological University,
Singapore
tranhavu@khu.ac.kr*

Abstract—Time reversal (TR) beamforming, considered as one of most prominent linear precoders, has showed the feasibility in conventional communications. In this paper, we propose the TR-based transmit optimization for heterogeneous networks (HetNets) where multiple femtocells apply TR precoders over frequency selective channels, with the signal-to-interference-plus-noise ratio (SINR) and interference constraints at single-antenna femtocell user devices. In multi-femtocell network environments, we exhibit that TR outperforms the well-known zero-forcing beamforming. Particularly, we focus on the practical case of imperfect channel estimation at femtocell base stations. The robust optimization methodology is hence devised by taking into account the average effect of channel estimation error (CEE) on system performance. Under the assumption of estimation error in time-varying channels, we derive the exact closed-form expressions of the desired signal, inter-symbol interference (ISI), inter-user interference (IUI), co- and cross-layer interference terms, respectively. These derivations allow us to tackle the proposed robust algorithm by convex optimization techniques. In final, numerical results are shown to confirm the validation of our proposal.

Index Terms—Heterogeneous network, beamforming, optimization, time reversal, channel estimation error, SINR.

I. INTRODUCTION

The growths of energy demand and restricting electromagnetic pollution lead to the motivations of green communications [1]–[3]. In [1], the authors indicated that the number of base stations (BSs) is more than 4 million and each BS consumes an average of 25 MWh per year (approximately 57 percent of total consumption of cellular network). Bearing in mind the environmental aspect, this causes a large amount of carbon footprint of operation in cellular networks. Otherwise, in 3GPP long-term evolution-advanced (LTE-A), the carrier aggregation technique now can provide a maximum bandwidth of 100 MHz [4]. With a much wider

bandwidth, the transmission also naturally suffers from the frequency-selective propagation effects. To deal with ISI and minimizing transmit power problems, previous works [5], [6] provided transmit beamforming algorithms under assumptions of receivers equipped appropriate equalizers and multiple antennas. Nevertheless, the high cost and complex equipment are non-preferred.

TR technique [7], [8], which possesses the focalization characteristic that is equivalent to the diversity gain, can provide the solution for mentioned problems. Evaluated as one of most prominent linear precoders, TR has been employed in many applications such as green communication, ultra-wideband (UWB) and large-scale antenna systems [3], [7]–[16]. By utilizing the joint time-reversed and conjugated form of channel impulse response (CIR) for prefiltering transmit signals to exploit multipath fading effects, the most signal energy of all paths is focused in the time and space domains at the receiver side. While UWB well matches TR because of the very high resolution in the channel estimation, it is more difficult to attain the accurate CIR in conventional bandwidth systems. The low resolution of channel estimation may induce the scaling down of focusing property, and the validation of employing TR in the conventional transmission should be evaluated. A measurement-based investigation on TR was carried out with 10 MHz bandwidth centred at 2.14 GHz which is comparable to the standard of 3G WCDMA systems in [15]. Its results reveal the potential capabilities of temporal and spatial focusing property. Moreover, the experimental results in [16] have confirmed the validity of TR properties (i.e. focusing gain and increased average received power) in conventional bandwidths. The feasibility of TR applications in 3GPP LTE-A coordinated multi-point networks was also mentioned in [7]. Therefore, these experimental and theoretical evidences imply the potential of TR in the broadband HetNet communications.

A number of recent works have addressed the designs of TR-based beamformer [8]–[13]. An earlier paper of research [8] showed SINR analysis in term of conventional TR prefilter over the channel model with exponential power

decay. M. Yoon *et al.* [11] establishes an optimization problem for combining TR beamformer and the minimum inter-symbol interference (MISI) prefilter to improve bit error rate (BER) performance. In the work [11], the authors have presented the optimal TR waveform, and the power loading policy is studied with the weighted sum-rate optimization problem for multi-user networks. In fact, most of previous works have been mainly carried out under perfect channel estimation. There have been no prior works on joint TR beamforming and power allocation with CEE for TR multi-user networks, whereas the effect of CEE on TR-based system performance is a greatly desirable problem [7], [13].

In this study, we speculate on the HetNet consisting of a macrocell base station (MBS), K femtocell stations (FBSs) and their users equipped a single tap diversity combiner. We are interested in proposing the conventional TR prefilter in term of transmit optimization for multi-femtocell network and then compare TR to zero-forcing beamforming. Moreover, we develop a novel *robust optimization methodology* for TR-based systems when the estimated channel may not be accurate due to the insufficient time and bandwidth over fast fading environments practically. Although the robust downlink beamforming designs under channel state information (CSI) errors have received desirable attention especially with the worst possible error case [17]–[18], this approach frequently leads to be pessimistic. Instead of analyzing the worst case optimization design, we show a more realistic methodology to guarantee the user experience by taking into account the average effects of CEE. The main challenge lies in the achieving of the closed-form expressions of the desired signal, ISI, IUI, co- and cross-layer interference terms under CEE effects over time-varying channels, while the prior analysis [8] is invalid. Based on derived analysis, we tackle the proposed robust algorithm by convex optimization technique. In final, the outperformance of TR reveals it in a more promising candidate than zero-forcing beamformer for green two-tier HetNets. And the effectiveness of our robust methodology is deliberated with Monte-Carlo simulation.

II. SYSTEM DESCRIPTION

We consider a two-tier HetNet system that includes one MBS and K TR-employed FBSs where MBS serves N_0 macrocell users (MUEs) and the k -th FBS communicates N_k femtocell users (FUEs) through a shared spectrum during transmission of MBS and FBSs. We suppose that user devices are equipped with one antenna and a single tap diversity combiner. An illustration of the network model is depicted in Fig. 1. For convenient notation, we denote the MBS as BS 0 and the k -th FBS as BS k ($k \geq 1$) respectively, and M_k antennas is equipped at BS k . In the multi-path channel model, the maximum length of each channel impulse response is equal to L . Thus, $\mathbf{h}_{ij}^{tr} \in \mathbb{C}^{L \times 1}$ ($0 \leq i \leq M_t$, $0 \leq j \leq N_r$) presents the CIRs between the i -th transmit antenna of BS t and the j -th user of BS r . Moreover, for notational convenience, we use superscript k to briefly represent superscript kk (i.e. \mathbf{h}_{ij}^{kk} can be replaced by \mathbf{h}_{ij}^k).

In communication systems, the designed precoder can be

decomposed into the emitted energy and phase rotation components. Considering the cases of frequency selective fading channel, the power allocation and beamforming algorithm can be separated into distinct processes. Thereupon, the transmit signals at the k -th FBS forwarding to its the j -th FU can be written by

$$\mathbf{x}_j^k = \sqrt{p_j^k} \left[\mathbf{g}_{0j}^k \quad \dots \quad \mathbf{g}_{M_k j}^k \right]^T s_j^k, \quad (1)$$

where s_j^k is the conveyed signal intended to its j -th FU from the k -th FBS, $\mathbf{p}^k = \left[\sqrt{p_1^k} \quad \sqrt{p_2^k} \quad \dots \quad \sqrt{p_{N_k}^k} \right]^T$ is defined as the transmit power vector of the k -th FBS, and $\mathbf{g}_{ij}^k \in \mathbb{C}^{L \times 1}$ can be considered as the beamforming vector used at the i -th transmit antenna of the k -th FBS for the j -th FU. Note that the time-reversed form of CIR is utilized as a matched-filter to prefilter message-bearing signals which is represented as

$$\mathbf{g}_{ij}^k[l] = \mathbf{h}_{ij}^{*k}[L+1-l] / \sqrt{\sum_{i=1}^M \|\mathbf{h}_{ij}^{kr}\|^2}. \quad (2)$$

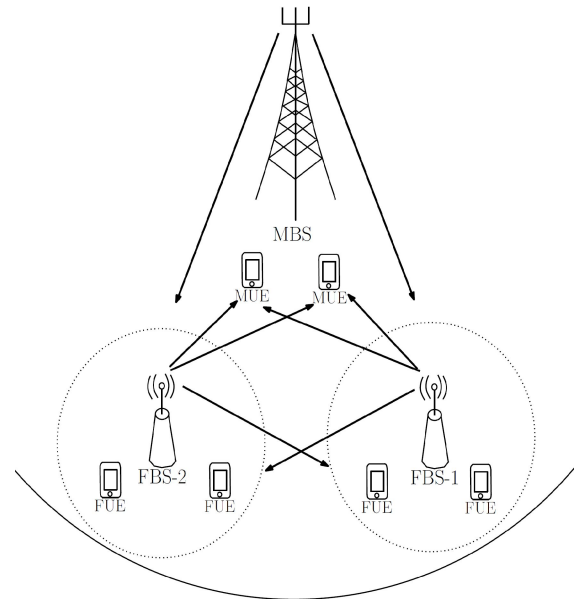


Fig. 1. A two-tier system model including a macrocell and two femtocells.

Let \mathbf{G}_{ij}^{kr} is $(2L-1) \times L$ Toeplitz matrix form of \mathbf{g}_{ij}^{kr} . Based on the representation of convolution in Toeplitz matrix form, the received signal at the j -th FU of the k -th FBS can be expressed as below

$$\mathbf{y}_j^k = \sum_{i=1}^{M_k} \sqrt{p_j^k} \mathbf{G}_{ij}^k \mathbf{h}_{ij}^k s_j^k + \sum_{\substack{j'=1 \\ j' \neq j}}^{N_k} \sum_{i=1}^{M_k} \sqrt{p_{j'}^k} \mathbf{G}_{ij}^k \mathbf{h}_{ij}^k s_{j'}^k + \sum_{\substack{r=1 \\ r \neq k}}^K \sum_{q=1}^{N_r} \sum_{i=1}^{M_q} \sqrt{p_q^r} \mathbf{G}_{iq}^r \mathbf{h}_{ij}^r s_q^r + \sum_{n=1}^{N_0} \sum_{m=1}^{M_0} \sqrt{p_n^0} \mathbf{U}_{mn} \mathbf{h}_{mj}^0 s_n^0 + \mathbf{n}_F, \quad (3)$$

where \mathbf{n}_F is Gaussian noise, the first term is the obtained signal for the j -th FU, the second term is interference in a

same femtocell, the third term is co-tier interference caused by other femtocells and the fourth term is the cross-tier interference from the MBS. \mathbf{U}_{mn} is $(2L-1) \times L$ Toeplitz

matrix form of \mathbf{u}_{mn} which is beamforming vector for the n -th MU at the m -th antenna of MBS. Then the SINR at the j -th FU belonging to the k -th FBS can be calculated in (4)

$$\text{SINR}_j^k \left(\mathbf{p}^k, \left\{ \hat{\mathbf{G}}_{ij}^k \right\}_{i=1, j=1}^{M_k, N_k} \right) = \frac{\left\| \sum_{i=1}^{M_k} \sqrt{p_j^k} (\mathbf{G}_{ij}^k \mathbf{h}_{ij}^k) [L] \right\|^2}{\underbrace{\sum_{l \neq L} \sum_{i=1}^{M_k} \left\| \sqrt{p_j^k} (\mathbf{G}_{ij}^k \mathbf{h}_{ij}^k) [l] \right\|^2}_{P_{(isi)_j^k}} + \underbrace{\sum_{j \neq j} \sum_{i=1}^{M_k} \left\| \sqrt{p_j^k} \mathbf{G}_{ij}^k \mathbf{h}_{ij}^k \right\|^2}_{P_{(iui)_j^k}} + \underbrace{\sum_{r=1}^K \sum_{q=1}^{N_r} \left\| \sum_{i=1}^{M_k} \sqrt{p_q^r} \mathbf{G}_{iq}^r \mathbf{h}_{ij}^{rk} \right\|^2}_{P_{(co)_j^k}} + \underbrace{\sum_{n=1}^{N_0} \left\| \sum_{m=1}^{M_0} \sqrt{p_n^0} \mathbf{U}_{mn} \mathbf{h}_{mj}^{0k} \right\|^2}_{P_{(cross)_j^k}} + \|\mathbf{n}_F\|^2}, \quad (4)$$

where $P_{(sig)_j^k}$, $P_{(isi)_j^k}$, $P_{(iui)_j^k}$, $P_{(co)_j^k}$ and $P_{(cross)_j^k}$ represent the desired signal, ISI, IUI, co-tier and cross-tier interference power, respectively.

III. NON-ROBUST AND ROBUST OPTIMIZATION PROBLEMS FOR TR FEMTOCELL NETWORKS

In this section, the distributed power loading strategy, in which each FBS only requires the local CSI and some of needed CSI from other BSs, is implemented. Since BSs are connected each other via backhaul connections, we suppose that each BS computes the interference power which it causes to neighbor MUs/FUs based on its current CSI, beamforming and power allocation vector, and then forwards this information to concerning BSs. In other words, each femtocell can know $P_{(co2)_j^k}$ and $P_{(cross)_j^k}$. Otherwise, the main victims of cross-tier interference are MUs because of sharing frequency spectrum between femtocell and macrocell networks, nevertheless, they have a strictly greater priority than FUs. To be specific for MUs's priority, femtocells therefore allocate the radiated power with the cross-tier interference constraint for MUs whereas the objective function aims at minimizing the total interference. With the perfect channel estimation, the downlink power control problem can be constituted with the tolerable level of cross-interference per each user $P_{(tol)_j}^{0k}$ and the preset threshold for SINR χ_j^k as

$$\begin{aligned} & \text{minimize } \left\{ \mathbf{p}^k \right\}_{k=1}^{N_k} \left(\sum_{j=1}^{N_k} \left(\sum_{n=1}^{N_0} \left\| \sum_{i=1}^{M_k} \mathbf{G}_{ij}^k \mathbf{h}_{in}^{k0} \right\|^2 + \sum_{r=1}^K \sum_{q=1}^{N_r} \left\| \sum_{i=1}^{M_k} \mathbf{G}_{ij}^k \mathbf{h}_{iq}^{rk} \right\|^2 \right) p_j^k \right), \\ & \text{subject to } \text{SINR}_j^k \left(\mathbf{p}^k, \left\{ \mathbf{G}_{ij}^k, \mathbf{h}_{ij}^k \right\}_{i=1, j=1}^{M_k, N_k} \right) \geq \chi_j^k, \\ & \left\| \sum_{i=1}^{M_k} \mathbf{G}_{ij}^k \mathbf{h}_{in}^{k0} \sqrt{p_j^k} \right\|^2 \leq P_{(tol)_j}^{k0}, \quad (1 \leq k \leq N_k). \end{aligned} \quad (5)$$

In general, the optimization design with SINR and interference constraints is the well-known non-convex formulation [5], [17], [19]. Because the beamformer has been determined by TR waveform, the problem (5) becomes convex second order cone program (SOCP) and it can be conveniently solved by convex optimization algorithms [20].

In reality, the focalization property of TR, which directly relates to system performance, decreases in case of CEE existence [7]. This practical case is specifically studied by making allowance for uncertainty errors in estimated femtocell channels and the imperfect CIR model is referred as

$$\hat{\mathbf{h}}_{ij}^{kr} = \mathbf{h}_{ij}^{kr} + \mathbf{e}_{ij}^{kr}, \quad (6)$$

in which $\hat{\mathbf{h}}_{ij}^{kr}$, \mathbf{h}_{ij}^{kr} and \mathbf{e}_{ij}^{kr} represent the estimated channel, true channel and estimation error, respectively. In fact, the true channel \mathbf{h}_{ij}^{kr} is a deterministic, however, unknown parameter. Thus, in our model, we assume that each tap of \mathbf{h}_{ij}^{kr} is independent circular symmetric complex Gaussian random variable with zero mean and variance as

$$\mathbb{E} \left[\left\| \mathbf{h}_{ij}^{kr} [l] \right\|^2 \right] = \langle \kappa \mathbb{E} \left[\left\| \hat{\mathbf{h}}_{ij}^{kr} [l] \right\|^2 \right] \rangle = \langle \kappa \uparrow_{krij,l}^2 \rangle, \quad (7)$$

where $(0 < \langle \kappa \rangle < 1)$, $\mathbb{E}[\cdot]$ denotes the expectation operator. We also suppose that \mathbf{h}_{ij}^{kr} and \mathbf{e}_{ij}^{kr} are identically independently distributed variables, and then we can write

$$\mathbb{E} \left[\left\| \mathbf{e}_{ij}^{kr} [l] \right\|^2 \right] = (1 - \langle \kappa \rangle) \uparrow_{krij,l}^2, \quad (8)$$

and $\hat{\mathbf{g}}_{ij}^{kr}$, the imperfect beamforming vector, is presented as

$$\hat{\mathbf{g}}_{ij}^{kr} [l] = \hat{\mathbf{h}}_{ij}^{*kr} [L+1-l] / \sqrt{\sum_{i=1}^M \left\| \hat{\mathbf{h}}_{ij}^{kr} \right\|^2}. \quad (9)$$

In practice, the information of estimated channel is stored and further updated at femtocells. At a time instant, the value of $\hat{\mathbf{h}}_{ij}^{kr}$ is treated as a constant vector while \mathbf{h}_{ij}^{kr} is unknown. By taking into account the average effects of CEE, the robust optimization methodology to guarantee QoS requirement is devised as

$$\text{minimize } \left\{ \mathbf{p}^k \right\}_{k=1}^{N_k} \mathbb{E}_{\mathbf{h}} \left[\sum_{j=1}^{N_k} \left(\sum_{n=1}^{N_0} \left\| \sum_{i=1}^{M_k} \hat{\mathbf{G}}_{ij}^k \mathbf{h}_{in}^{k0} \right\|^2 + \sum_{r=1}^K \sum_{q=1}^{N_r} \left\| \sum_{i=1}^{M_k} \hat{\mathbf{G}}_{ij}^k \mathbf{h}_{iq}^{rk} \right\|^2 \right) p_j^k \right],$$

$$\text{subject to } E_{\mathbf{h}} \left[\text{SINR}_j^k \left(\mathbf{p}^k, \left\{ \hat{\mathbf{G}}_{ij}^k \right\}_{i=1, j=1}^{M_k, N_k} \right) \right] \geq \chi_j^k, \quad (10)$$

$$E_{\mathbf{h}} \left[\left\| \sum_{i=1}^{M_k} \hat{\mathbf{G}}_{ij}^k \mathbf{h}_{in}^{k0} \sqrt{P_j^k} \right\|^2 \right] \leq P_{(tol)n}^{k0},$$

where ($1 \leq k \leq N_k$), and in which $E_{\mathbf{h}}[\cdot]$ denotes briefly for the expectation on the channel variables. In fact, the above problem is intractable because we have no closed-form derivations of objective function as well as constraints. To make problem (10) solvable, the analysis for the objective function as well as the left-side part of constraints need to be derived. Nevertheless, it is very difficult (if not impossible) to obtain directly the exact expectation of SINR, we can well approximate it by computing the expression as in [8]

$$E_{\mathbf{h}} \left[\text{SINR}_j^k \left(\mathbf{p}^k, \left\{ \hat{\mathbf{G}}_{ij}^k \right\}_{i=1, j=1}^{M_k, N_k} \right) \right] \approx \frac{E_{\mathbf{h}} \left[P_{(sig)j}^k \right]}{E_{\mathbf{h}} \left[P_{(isi)j}^k + P_{(iui)j}^k + P_{(co)j}^k + P_{(cross)j}^k \right] + \|\mathbf{n}_F\|^2}. \quad (11)$$

Theorem 1: Following given assumptions of error model, the closed-form expressions of objective function as well as the left-side part of constraints in optimization problem (10) can be given by:

$$E_{\mathbf{h}} \left[P_{(sig)j}^k \right] = p_j \frac{\sum_{i=1}^{M_k} \left(\sum_{l=1}^L (1-\langle k \rangle) \uparrow_{kij,l}^4 + \left(\sum_{l=1}^L |\hat{\mathbf{h}}_{ij}^{*k}[l]|^2 - (1-\langle k \rangle) \uparrow_{kij,l}^2 \right)^2 \right)}{\sum_{i=1}^{M_k} \sum_{l=1}^L |\hat{\mathbf{h}}_{ij}^k[l]|^2} + \frac{\sum_{i=1}^{M_k} \sum_{l=1}^L \sum_{l'=1}^L \left(|\hat{\mathbf{h}}_{ij}^{*k}[l]|^2 - (1-\langle k \rangle) \uparrow_{kij,l}^2 \right) \left(|\hat{\mathbf{h}}_{ij}^{*k}[l']|^2 - (1-\langle k \rangle) \uparrow_{kij,l'}^2 \right)}{\sum_{i=1}^{M_k} \sum_{l=1}^L |\hat{\mathbf{h}}_{ij}^k[l]|^2}. \quad (12)$$

$$E_{\mathbf{h}} \left[P_{(isi)j}^k \right] = p_j \sum_{z=1}^{L-1} \left(\frac{\sum_{i=1}^{M_k} \sum_{l=1}^L \left(\|\hat{\mathbf{h}}_{ij}^k[z+1-l]\|^2 \uparrow_{kij,L+1-l}^2 + \|\hat{\mathbf{h}}_{ij}^k[L-z+l]\|^2 \uparrow_{kij,l}^2 \right)}{\sum_{m=1}^{M_k} \sum_{l=1}^L |\hat{\mathbf{h}}_{ij}^{kr}[l]|^2} \right). \quad (13)$$

$$E_{\mathbf{h}} \left[P_{(iui)j}^k \right] = \sum_{j \neq j}^{N_r} p_j^k \Xi \left(\hat{\mathbf{G}}_{ij}^k, \mathbf{h}_{ij}^k \right), \quad (14)$$

$$E_{\mathbf{h}} \left[\left\| \sum_{j=1}^{N_k} \left(\sum_{n=1}^{N_0} \left\| \sum_{i=1}^{M_k} \hat{\mathbf{G}}_{ij}^k \mathbf{h}_{in}^{k0} \right\|^2 + \sum_{r=1}^K \sum_{q=1}^{N_r} \left\| \sum_{i=1}^{M_k} \hat{\mathbf{G}}_{ij}^k \mathbf{h}_{iq}^{kr} \right\|^2 \right) \right\|^2 \right] = \sum_{j=1}^{N_k} \left(\sum_{n=1}^{N_0} \Xi \left(\hat{\mathbf{G}}_{ij}^k, \mathbf{h}_{in}^{k0} \right) + \sum_{r=1}^K \sum_{q=1}^{N_r} \Xi \left(\hat{\mathbf{G}}_{ij}^k, \mathbf{h}_{iq}^{kr} \right) \right), \quad (15)$$

$$E_{\mathbf{h}} \left[\left\| \sum_{i=1}^{M_k} \hat{\mathbf{G}}_{ij}^k \mathbf{h}_{in}^{k0} \right\|^2 \right] = \Xi \left(\hat{\mathbf{G}}_{ij}^k, \mathbf{h}_{in}^{k0} \right), \quad (16)$$

where

$$\Xi \left(\hat{\mathbf{G}}_{ij}^k, \mathbf{h}_{mn}^{kt} \right) = \langle k \rangle \left(\frac{\sum_{i=1}^{M_k} \sum_{l=1}^L |\hat{\mathbf{h}}_{ij}^{kr}[l]|^2 \uparrow_{kmn,l}^2 + \sum_{k=1}^{L-1} \left(\frac{\sum_{i=1}^{M_k} \sum_{l=1}^L \left(|\hat{\mathbf{h}}_{ij}^{kr}[z+1-l]|^2 \uparrow_{kmn,L+1-l}^2 + |\hat{\mathbf{h}}_{ij}^{kr}[L-z+l]|^2 \uparrow_{kmn,l}^2 \right)}{\sum_{i=1}^{M_k} \sum_{l=1}^L |\hat{\mathbf{h}}_{ij}^{kr}[l]|^2} \right)}{\sum_{i=1}^{M_k} \sum_{l=1}^L |\hat{\mathbf{h}}_{ij}^{kr}[l]|^2} \right). \quad (17)$$

Proof: First of all, we consider $P_{(sig)j}^k$ term. The central tap in equivalent channel $(\hat{\mathbf{G}}_{ij}^k \mathbf{h}_{ij}^k)$ is evaluated as the signal component. Thanks to TR, the difference between the main tap and the other taps is enhanced. However, the CEE effect induces a reduction on focusing property of central tap and its expectation is then analysed as follows

$$E_{\mathbf{h}} \left[\left| \sum_{i=1}^{M_k} (\hat{\mathbf{G}}_{ij}^k \mathbf{h}_{ij}^k)[L] \right|^2 \right] = E_{\mathbf{h}} \left[\sum_{i=1}^{M_k} \left| (\hat{\mathbf{G}}_{ij}^k \mathbf{h}_{ij}^k)[L] \right|^2 + \text{Re} \left\{ \sum_{\substack{i'=1 \\ i' \neq i}}^{M_k} \sum_{i=1}^{M_k} (\hat{\mathbf{G}}_{ij}^k \mathbf{h}_{ij}^k)[L] (\hat{\mathbf{G}}_{i'j}^k \mathbf{h}_{i'j}^k)[L] \right\} \right]. \quad (18)$$

We separate the right-side into two components. To solve the first term of the left-side, we focus on

$$E_{\mathbf{h}} \left[\sum_{i=1}^{M_k} \left| (\hat{\mathbf{G}}_{ij}^k \mathbf{h}_{ij}^k)[L] \right|^2 \right] = E_{\mathbf{h}} \left[\sum_{i=1}^{M_k} \left(\sum_{l=1}^L |\hat{\mathbf{h}}_{ij}^{*k}[l] \mathbf{h}_{ij}^k[l]|^2 + \text{Re} \left\{ \sum_{\substack{l'=1 \\ l' \neq l}}^L \sum_{i=1}^{M_k} \hat{\mathbf{h}}_{ij}^{*k}[l] \mathbf{h}_{ij}^k[l] \hat{\mathbf{h}}_{ij}^{*k}[l'] \mathbf{h}_{ij}^k[l'] \right\} \right) \right]. \quad (19)$$

in which, we obtain results after algebraic derivations that

$$E_{\mathbf{h}} \left[|\hat{\mathbf{h}}_{ij}^{*k}[l] \mathbf{h}_{ij}^k[l]|^2 \right] = E_{\mathbf{e}} \left[\left| \hat{\mathbf{h}}_{ij}^{*k}[l] (\hat{\mathbf{h}}_{ij}^k[l] - \mathbf{e}_{ij}^k[l]) \right|^2 \right] = \left(|\hat{\mathbf{h}}_{ij}^k[l]|^2 - (1-\langle k \rangle) \uparrow_{kij,l}^2 \right)^2 + (1-\langle k \rangle) \uparrow_{kij,l}^4, \quad (20)$$

and

$$E_{\mathbf{h}} \left[\sum_{\substack{l'=1 \\ l' \neq l}}^L \sum_{i=1}^{M_k} \hat{\mathbf{h}}_{ij}^{*k}[l] \mathbf{h}_{ij}^k[l] \hat{\mathbf{h}}_{ij}^{*k}[l'] \mathbf{h}_{ij}^k[l'] \right] = \sum_{l'=1}^L \sum_{l=1}^L \left(|\hat{\mathbf{h}}_{ij}^{*k}[l]|^2 - (1-\langle k \rangle) \uparrow_{kij,l}^2 \right) \left(|\hat{\mathbf{h}}_{ij}^{*k}[l']|^2 - (1-\langle k \rangle) \uparrow_{kij,l'}^2 \right). \quad (21)$$

Continuously, the second term of the left-side of (18) can be expressed as

$$E_{\mathbf{h}} \left[\sum_{\substack{i'=1 \\ i' \neq i}}^{M_k} \sum_{i=1}^{M_k} (\hat{\mathbf{G}}_{ij}^k \mathbf{h}_{ij}^k)[L] (\hat{\mathbf{G}}_{i'j}^k \mathbf{h}_{i'j}^k)[L] \right] =$$

$$= \sum_{i \neq l}^{M_k} \sum_{i=1}^{M_k} \sum_{l=1}^L \left(\left| \hat{\mathbf{h}}_{ij}^{*k} [l] \right|^2 - (1-\zeta^k) \uparrow_{kij,l}^2 \right) \left(\left| \hat{\mathbf{h}}_{ij}^{*k} [l] \right|^2 - (1-\zeta^k) \uparrow_{ki,j,l}^2 \right). \quad (22)$$

Inserting (20)–(22) into (18), the closed-form expression of signal component can be written as (12).

Consequently, in TR-based transmissions, the power of ISI

component can be given by $E \left[\sum_{z=1}^{2L-1} \sum_{i=1}^{M_k} \left(\hat{\mathbf{G}}_{ij}^k \mathbf{h}_{ij}^k \right) [z] \right]^2$. Let us

consider $E \left[\sum_{i=1}^{M_k} \left(\hat{\mathbf{G}}_{ij}^k \mathbf{h}_{ij}^k \right) [z] \right]^2$ for simplicity, herein, we

express it in a similar way to (18). Moreover, we infer that

$$\begin{aligned} & \sum_{i=1}^{M_k} E \left[\left(\hat{\mathbf{G}}_{ij}^k \mathbf{h}_{ij}^k \right) [z] \right]^2 = \\ & = \frac{\sum_{i=1}^{M_k} \sum_{l=1}^z \zeta_k \left\| \hat{\mathbf{h}}_{ij}^k [z+1-l] \right\|^2 \uparrow_{kij,L+1-l}^2}{\sum_{i=1}^{M_k} \sum_{l=1}^L \left| \hat{\mathbf{h}}_{ij}^k [l] \right|^2}, \quad (23) \end{aligned}$$

and

$$E_{\mathbf{h}} \left[\sum_{i=1}^{M_k} \sum_{i \neq j}^{M_k} \left(\hat{\mathbf{G}}_{ij}^k \mathbf{h}_{ij}^k \right) [z] \left(\hat{\mathbf{G}}_{ij}^{*k} \mathbf{h}_{ij}^{*k} \right) [z] \right] = 0. \quad (24)$$

From (23) and (24), the expectation of $P_{(isi)_j}^k$ can be calculated as (13).

In the next, the fact is that the key of the evaluations of (14)–(16) lies in (17). Hence, to analyse (17), we separate it into three parts as follows

$$\begin{aligned} \Xi \left(\hat{\mathbf{G}}_{ij}^{kr}, \mathbf{h}_{mn}^{kt} \right) &= E_{\mathbf{h}} \left[\sum_{z=1}^{L-1} \sum_{i=1}^{M_k} \hat{\mathbf{G}}_{ij}^{kr} \mathbf{h}_{mn}^{kt} [z] \right]^2 + \\ &+ E_{\mathbf{h}} \left[\sum_{i=1}^{M_k} \hat{\mathbf{G}}_{ij}^{kr} \mathbf{h}_{mn}^{kt} [L] \right]^2 + \\ &+ E_{\mathbf{h}} \left[\sum_{z=L+1}^{2L-1} \sum_{i=1}^{M_k} \hat{\mathbf{G}}_{ij}^{kr} \mathbf{h}_{mn}^{kt} [z] \right]^2. \quad (25) \end{aligned}$$

By utilizing manipulations similar to the signal and ISI terms, (17) can be achieved by below expressions

$$\begin{aligned} & E_{\mathbf{h}} \left[\sum_{i=1}^{M_k} \hat{\mathbf{G}}_{ij}^{kr} \mathbf{h}_{mn}^{kt} [L] \right]^2 = \\ & = \zeta_k \left(\sum_{k=1}^{L-1} \frac{\sum_{i=1}^{M_k} \sum_{l=1}^L \left| \hat{\mathbf{h}}_{ij}^{kr} [l] \right|^2 \uparrow_{ktmn,l}^2}{\sum_{i=1}^{M_k} \sum_{l=1}^L \left| \hat{\mathbf{h}}_{ij}^{kr} [l] \right|^2} \right), \quad (26) \end{aligned}$$

$$E_{\mathbf{h}} \left[\sum_{z=1}^{L-1} \sum_{i=1}^{M_k} \hat{\mathbf{G}}_{ij}^{kr} \mathbf{h}_{mn}^{kt} [z] \right]^2 =$$

$$= \zeta_k \sum_{k=1}^{L-1} \left(\frac{\sum_{i=1}^{M_k} \sum_{l=1}^z \left(\left| \hat{\mathbf{h}}_{ij}^{kr} [z+1-l] \right|^2 \uparrow_{ktmn,L+1-l}^2 \right)}{\sum_{i=1}^{M_k} \sum_{l=1}^L \left| \hat{\mathbf{h}}_{ij}^{kr} [l] \right|^2} \right), \quad (27)$$

$$E_{\mathbf{h}} \left[\sum_{z=L+1}^{2L-1} \sum_{i=1}^{M_k} \hat{\mathbf{G}}_{ij}^{kr} \mathbf{h}_{mn}^{kt} [z] \right]^2 =$$

$$= \zeta_k \left(\sum_{k=1}^{L-1} \frac{\sum_{i=1}^{M_k} \sum_{l=1}^z \left(\left| \hat{\mathbf{h}}_{ij}^{kr} [L-z+l] \right|^2 \uparrow_{ktmn,l}^2 \right)}{\sum_{i=1}^{M_k} \sum_{l=1}^L \left| \hat{\mathbf{h}}_{ij}^{kr} [l] \right|^2} \right). \quad (28)$$

Based on (12)–(17), we can predict the instantaneous SINR performance under the average effect of CEE. The validity of our analyses is justified by Monte-Carlo simulations in the numerical result section.

In light of *Theorem 1*, we therefore relax the problem (10) into the robust optimization problem described as below

$$\begin{aligned} & \underset{\{\mathbf{p}^k\}_{k=1}^{N_k}}{\text{minimize}} \sum_{j=1}^{N_0} \sum_{n=1}^{N_0} \Xi \left(\hat{\mathbf{G}}_{ij}^k, \mathbf{h}_m^{k0} \right) + \sum_{r=1}^K \sum_{q=1}^{N_r} \sum_{r \neq k} \Xi \left(\hat{\mathbf{G}}_{ij}^k, \mathbf{h}_{iq}^{kr} \right) p_j^k, \\ & \text{subject to} \frac{E_{\mathbf{h}} \left[P_{(sig)_j}^k \right]}{E_{\mathbf{h}} \left[P_{(isi)_j}^k + P_{(iii)_j}^k + P_{(co)_j}^k + P_{(cross)_j}^k \right] + \|\mathbf{n}_F\|^2} \geq x_j^k, \quad (29) \\ & \Xi \left(\hat{\mathbf{G}}_{ij}^k, \mathbf{h}_m^{k0} \right) p_j^k \leq P_{(tol)_n}^{k0}. \end{aligned}$$

where $(1 \leq k \leq N_k)$. Thus, the challenge is now overcome and the optimal solution can be obtained by CVX or SeDuMi solvers [20].

IV. NUMERICAL RESULTS

In order to assess the performance of our proposal, Monte Carlo simulation is carried out. In our model, we assume that the coverage radius of MBS and each FBS are 200 m and 10 m, respectively. FBSs are uniformly located in a circle of 100 m far from MBS, and MUs and FUs are uniformly located in the served area. The simulation is implemented in the ITU-R channel standard [21]. We set $\|\mathbf{n}_F\|^2 = 1$,

$$\left\{ x_j^k \right\}_{j=1}^{N_k} = x_F \text{ and } \left\{ P_{(cross)_j}^k \right\}_{j=1}^{N_k} = 0.01 \text{ for simplicity.}$$

First of all, under perfect channel estimation, we compare TR beamforming to the well-known zero-forcing scheme in multi-femtocell environments by problem (5) to show the effectiveness of our proposal. The zero-forcing waveform can be achieved by utilizing the manner similar to [9], [10], however, multiple transmit antennas and multiple users should be taken into account extensively. From Fig. 2, we can observe that the TR-applied system can save approximately a maximal power of 5 dBm and 4.5 dBm compared to zero-forcing beamforming when 1 and 2 femtocells are

considered, respectively. In turn, the beamforming scheme of zero-forcing outperforms that of TR at a SNR region which is larger than 1.8 dB. Nevertheless, the radiated power of FBS is limited up to 20 dBm in femtocell environments [2]. It means that TR beamforming technique can be evaluated as a more promising candidate than the very prominent zero-forcing for the future green HetNet.

TABLE I. SIMULATION PARAMETERS.

Number of antennas at MBS	4	Number of users at each FBS	2
Number of antennas at FBS	4	Pathloss exponent of outdoor, indoor and outdoor to indoor link	4, 3, 3.5
Number of users at MBS	2	$P_{(tol)n}^{k0}$	-5dBm

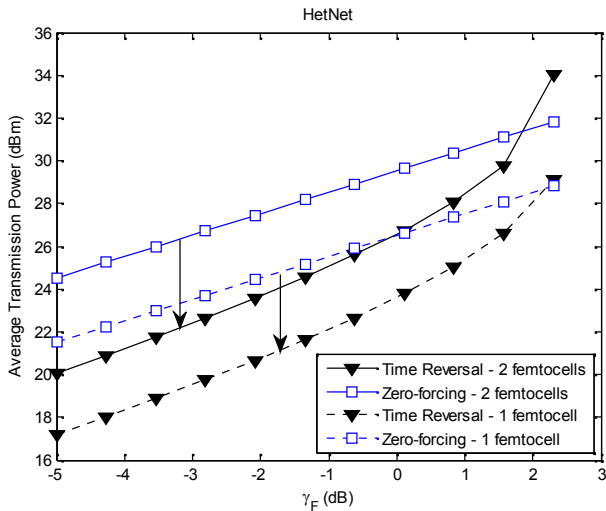


Fig. 2. Performance comparison between TR and zero-forcing.

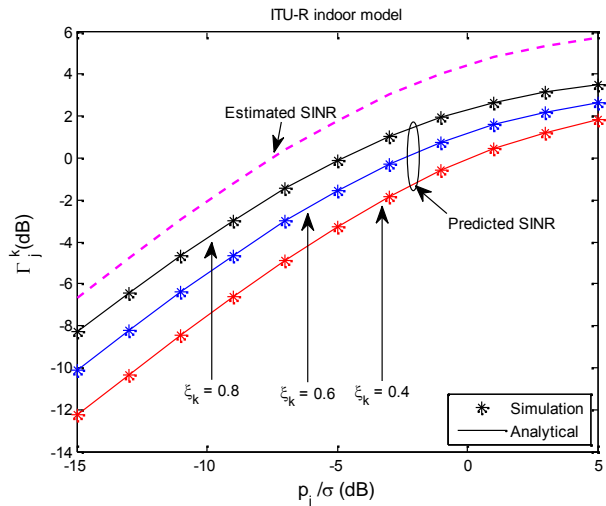


Fig. 3. Average effects of CEE over time-varying channels.

In the next, we verify the validations of *Theorem 1* in Fig. 3. Because the accuracy of (16) can be checked by evaluating the IUI component only, the analyses of *Theorem 1* are then jointly considered through SINR, nevertheless, without the co- and cross-layer interference components for conveniences. From the observations, we can see the well-agreement is achieved between the simulation and analytical results. Fig. 3 also indicates that the SINR performance scales down as a function of ξ_k due to the loss of focalization. Following this

theorem, we can predict the average effects of CEE on the system performance at a time instant.

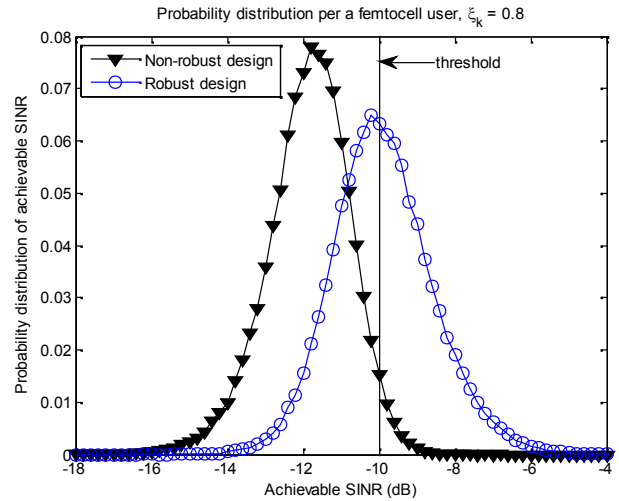


Fig. 4. Probability distribution of SINR per each FU.

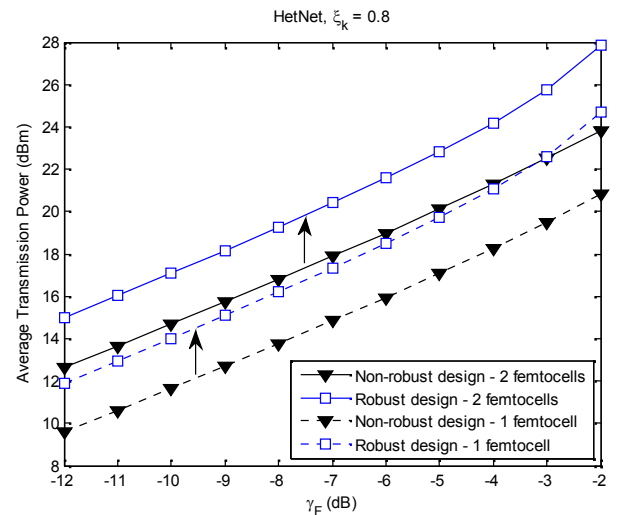


Fig. 5. Power performance trade-off of the robust design.

Figure 4 indicates the probability distribution of achievable SINR per an FU obtained by non-robust and robust design, in which we use 100000 randomly generated realizations for the simulation. Note that the non-robust design is strictly similar to problem (5), however, the notation of perfect values are appropriately replaced by estimated values. By a simple calculation of outage probability, it can be evaluated that our robust design can reduce significantly the outage probability from 96.43 % to 45.89% by accounting the expectation of CEE effects in case of $\xi_k = 0.8$. For the probability distribution of proposed robust methodology, we might see the mean position is located nearly the preset threshold. It can be explained that the methodology allocates the power based on the average effects of CEE and then the outage probability is improved up to 50 % roughly. Moreover, as a reference, we plot the average transmit power of non-robust and robust manner in Fig. 5 to exhibit how much additional power which is required to achieve the outage probability characterization.

V. CONCLUSIONS

This paper has proved for our proposal that TR technique conclusively comports with HetNet environments where

multiple femtocells are employed. Specifically, at working point of femtocell networks, TR reveals a desirable outperformance compared to zero-forcing beamforming technique. In the next, by taking into account CEE, we propose the novel robust optimization methodology to ensure the user experience under the imperfect CSI supposition. To tackle the robust problem, the closed-form SINR expression under the effects of time-varying channels needs to be derived. By overcoming this challenge, the robust problem is relaxed into a solvable convex optimization one. The simulation results depict that the proposed methodology significantly degrades the outage probability when CEE occurs. Thus, the outperformance of TR femtocell systems in two-tier HetNet exhibits that the mobile devices may obtain a very high multi-path diversity gain in saving power without any hardware upgrades at user devices. These delightful outcomes reveal the proposals in a bright approach.

REFERENCES

- [1] Z. Hasan, H. Boostanimehr, V. K. Bhargava, "Green cellular networks: A survey, some research issues and challenges", *IEEE Comm. Surveys & Tutorials*, vol. 13, no. 4, pp. 524–540, 2011. [Online]. Available: <http://dx.doi.org/10.1109/SURV.2011.092311.00031>
- [2] T. Zahir *et al.*, "Interference management in femtocells", *IEEE Comm. Surveys & Tutorial*, vol. 15, no. 1, pp. 293–311, 2013. [Online]. Available: <http://dx.doi.org/10.1109/SURV.2012.020212.00101>
- [3] B. Wang *et al.*, "Green wireless communications: A time-reversal paradigm", *IEEE Journal on Selected Areas in Communications*, vol. 29, no. 8, pp. 1698–1710, 2011. [Online]. Available: <http://dx.doi.org/10.1109/JSAC.2011.110918>
- [4] A. Bleicher, "4G gets real", *IEEE Spectrum*, vol. 51, no. 1, pp. 38–62, 2014. [Online]. Available: <http://dx.doi.org/10.1109/MSPEC.2014.6701430>
- [5] Farrokh Rashid-Farrokhi *et al.*, "Transmit beamforming and power control for cellular wireless systems", *IEEE Journal on Selected Areas in Communications*, vol. 16, no. 8, pp. 1437–1450, 1998. [Online]. Available: <http://dx.doi.org/10.1109/49.730452>
- [6] Yang-wen Liang *et al.*, "Transmit beamforming for frequency-selective channels with decision-feedback equalization", *IEEE Trans. on Wireless Comm.*, vol. 6, no. 12, pp. 4401–4411, 2007. [Online]. Available: <http://dx.doi.org/10.1109/TWC.2007.060256>
- [7] M.-A. Bouzigués *et al.*, "Turn back the clock: Time reversal for green radio communications", *IEEE Vehicular Technology Magazine*, vol. 8, no. 1, pp. 49–56, 2013. [Online]. Available: <http://dx.doi.org/10.1109/MVT.2012.2234054>
- [8] Feng Han *et al.*, "Time-reversal division multiple access over multi-path channels", *IEEE Trans. Communications*, vol. 60, no. 7, pp. 1953–1965, 2012. [Online]. Available: <http://dx.doi.org/10.1109/TCOMM.2012.051012.110531>
- [9] Vu Tran-Ha *et al.*, "Time reversal-based transmissions with distributed power allocation for two-tier networks", in *Proc. of 29-th Advanced Information Networking and Applications Workshops*, pp. 181 – 186, 2015. [Online]. Available: <http://dx.doi.org/10.1109/waina.2015.29>
- [10] H. Nguyen, Z. Zhao, F. Zheng, T. Kaiser, "Preequalizer design for spatial multiplexing SIMO-UWB TR systems", *IEEE Trans. Vehicular Communications*, vol. 59, no. 8, pp. 3798–3805, 2010. [Online]. Available: <http://dx.doi.org/10.1109/TVT.2010.2064345>
- [11] Misun Yoon, Chungyong Lee, "A TR-MISI serial prefilter for robustness to ISI and noise in indoor wireless communication system", *IEEE Signal Process. Letters*, vol. 21, no. 4, pp. 386–389, 2014. [Online]. Available: <http://dx.doi.org/10.1109/LSP.2014.2303814>
- [12] Y.-H. Yang, B. Wang, W. S. Lin, K. J. Ray Liu, "Near-optimal waveform design for sum rate optimization in time-reversal multiuser downlink systems", *IEEE Trans. Wireless Communications*, vol. 12, no. 1, pp. 346–357, 2013. [Online]. Available: <http://dx.doi.org/10.1109/TWC.2012.120312.120572>
- [13] G. C. Ferrante, J. Fiorina, M. G. Di Benedetto, "Statistical analysis of the SNR loss due to imperfect time reversal", in *Proc. of Int. Conf. on Ultra-wideband (ICUWB)*, pp. 36–40, 2014. [Online]. Available: <http://dx.doi.org/10.1109/icuwb.2014.6958947>
- [14] A. Pitarokoilis *et al.*, "Uplink performance of time-reversal MRC in massive MIMO systems subject to phase noise", *IEEE Trans. Wireless Communications*, vol. 14, no. 2, pp. 711–723, 2015. [Online]. Available: <http://dx.doi.org/10.1109/TWC.2014.2359018>
- [15] H. T. Nguyen *et al.*, "Time reversal in wireless communications: a measurement based investigation", *IEEE Trans. Wireless Communications*, vol. 5, no. 8, pp. 2242–2252, 2006. [Online]. Available: <http://dx.doi.org/10.1109/TWC.2006.1687740>
- [16] I. H. Naqvi *et al.*, "Robustness of a time reversal system: From ultra-wide to narrow bandwidths", in *Proc. of IEEE Wireless Comm. and Networking Conference (WCNC)*, pp. 37–41, 2012. [Online]. Available: <http://dx.doi.org/10.1109/wcnc.2012.6214394>
- [17] S. A. Vorobyov, A. B. Gershman, Z.-Q. Luo, "Robust adaptive beamforming using worst-case performance optimization: a solution to the signal mismatch problem", *IEEE Trans. Signal Processing*, vol. 51, no. 2, pp. 313–324, 2003. [Online]. Available: <http://dx.doi.org/10.1109/TSP.2002.806865>
- [18] S. Parsaeefard, M. van der Schaar, A. R. Sharafat, "Robust power control for heterogeneous users in shared unlicensed bands", *IEEE Trans. on Wireless Comm.*, vol. 13, no. 6, pp. 3167–3182, 2014. [Online]. Available: <http://dx.doi.org/10.1109/TWC.2014.042314.130981>
- [19] V. Chandrasekhar *et al.*, "Power control in two-tier femtocell networks", *IEEE Trans. Wireless Communications*, vol. 8, no. 8, pp. 4316–4328, 2009. [Online]. Available: <http://dx.doi.org/10.1109/TWC.2009.081386>
- [20] M. Grant, S. Boyd, *CVX: Matlab software for disciplined convex programming*. 2009. [Online]. Available: <http://www.stanford.edu/~boyd/cvx/>
- [21] IEEE Technical Report, "Channel models for TGS", 2012. [Online]. Available: <https://mentor.ieee.org/802.15/dcn/12/15-12-0459-06-0008-tg8-channel-models.doc>